

Testing of multispectral scanner data for prospecting of ferro-eclogite in the Førdefjord area, western Norway

BJØRN A. FOLLESTAD, ARE KORNELIUSSEN & NIGEL J. COOK

Follestad, B.A., Korneliussen, A. & Cook, N.J. 2000: Testing of multispectral scanner data for prospecting of ferro-eclogite in the Førdefjord area, Western Norway. *Norges geologiske undersøkelse Bulletin 436*, 193-201.

The present investigation aimed to determine whether remote sensing data can be used in future prospecting for rutile-bearing eclogite. A preliminary study was carried out to establish if the method is suitable for distinguishing different key rock types at Engebøfjell, western Norway, in which large volumes of rutile are hosted within ferro-eclogite. The study was carried out in three parts: laboratory measurement of reflectivity curves on representative samples, field measurement of samples using a portable spectral radiometer and spectral analysis of data collected with the airborne hyperspectral scanner. Both the laboratory and the field measurements indicated that the rock surfaces of ferro-eclogite generally have a lower reflectivity compared with the surfaces of both leuco-eclogite and gneiss. Different % reflectivity values in distinct parts of the spectrum can apparently be used as a tool to discriminate between areas characterised by gneiss, leuco-eclogite and ferro-eclogite. However, the presence of moss on the rock surface will change these characteristics significantly and make precise characterisation difficult. The airborne scanner testing was hampered in this study by the unavailability of those bands that proved useful for distinguishing eclogite types in the field and laboratory. However, they are useful in that they reveal a means to discriminate between vegetated and bare rock surfaces. The application of airborne measurement techniques and suitable data processing would appear to be a promising method with potential for routine application in prospecting. Application is, however, dependent upon the availability of channels for the instrumentation being more appropriate than in this study. Also, the considerable influence of vegetation and moss on the data would appear to be critical to successful implementation of the method.

Bjørn A. Follestad, Are Korneliussen & Nigel J. Cook, Geological Survey of Norway, N-7491 Trondheim, Norway.

Introduction

In 1996, a covenant agreement for testing the potential of the multispectral scanner technique as a prospecting tool in an area of Sogn & Fjordane county was established between the Sogn & Fjordane county administration (Department of Regional Policy) and the Geological Survey of Norway (NGU). The studies were related to on-going geological investigations in the Engebøfjell area in the Førdefjord district of western Norway (Fig. 1).

The Engebøfjell eclogite deposit is located on the northern side of Førdefjord near the small community of Vevring in Naustdal commune. The Førdefjord area belongs geologically to the Western Gneiss region, situated between the Devonian Kvamshesten Basin to the south and the Devonian Håsteinen Basin to the north. The Førdefjord region consists of a variety of amphibolitic, eclogitic and gabbroic rocks, together with tonalitic, dioritic and granitic gneisses. The Engebø eclogite is a 2.5 km-long, complexly deformed, lens-shaped body surrounded by alternating mafic and felsic country rocks (Korneliussen & Foslie 1985). The protolith to the eclogite is believed to be a Fe- and Ti-rich gabbro of Proterozoic age. Transformation into eclogite is related to Caledonian high-pressure metamorphism at ca. 400 Ma. During this process, ilmenite in the gabbro protolith was replaced by rutile. The eclogite body is subdivided into a leuco-eclogite and a ferro-eclogite variety. Ferro-eclogite, which is distinctly enriched in both Fe (>14% Fe₂O₃) and Ti (>3% TiO₂; primarily

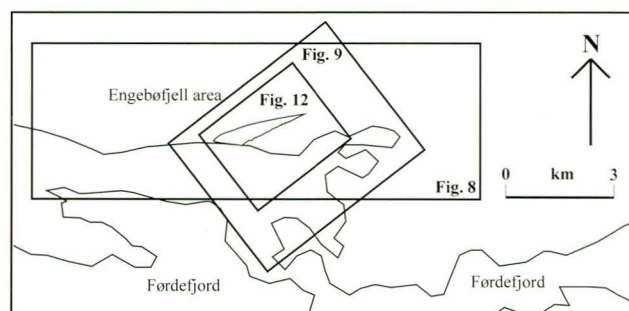


Fig. 1. Location of the Førdefjord district of western Norway and the area around Engebøfjell where the airborne multispectral scanner data were collected (Figs. 9 and 12). The eclogite area is shaded.

as rutile), has been the target for rutile exploration. This investigation addressed whether remote sensing data can be used in future prospecting for rutile-bearing eclogite of the Engebøfjell type.

Remote sensing as a prospecting method

Remote sensing technology applied to Earth resource monitoring and management has been employed on a global scale since the early 1970s when the first Earth Resource Satellite (ERS) was launched. This satellite, later renamed the

Landsat Earth resources satellite, was the first of a series of 6 satellites designed to provide a near-global coverage of the Earth's surface on a regular and predictable basis; Landsat 6 was, however, lost on launch. The return beam vidicon (RBV) which is a TV camera-like instrument, and the multispectral scanner (MSS) were the principal sensors on Landsat 1, 2 and 3. These instruments were operating in the ranges 0.4 - 0.8 and 0.5 - 1.1 μm , respectively. An additional thermal band 7 (10.3 - 12.6 μm) was added on Landsat 3 and the 3 RBV cameras were exchanged for 2 RBV cameras, offering improved resolution (see Richards & Jia 1999). The Thematic Mapper (TM), substituted for the RBV cameras, permitted improved spectral, spatial and radiometric scanner characteristics in Landsat 4 and 5. An additional band (7) in the 2.08 - 2.35 μm region was added to the six existing bands (1-6) at the request of the geological community, due to the importance of the 2 μm region in assessing hydrothermal alteration on the Earth's surface.

Multispectral line scanners have been available for civil aircraft since the early 1970s, and have contributed to the utilisation, understanding and interpretation of the scanner data obtained through Earth orbiting systems. These aircraft scanners, e.g., the Daedalus AADS 1240/1260 multispectral line scanners, operate in the ultraviolet, visible/reflective IR and the thermal parts of the spectrum, and permit data acquisition in 12 wavebands. Along with the Airborne Thematic Mapper (ATM), these airborne missions were used, for example, for simulation studies prior to the launch of Landsat 4. At 12 km altitude, the ATM airborne scanner produces an equivalent area pixel size on the ground (30 m) as the Landsat TM. The availability of new detector technologies made it possible, throughout the 1980s, to develop aircraft scanners capable of recording in a large number of spectral bands (Richards & Jia 1999). For example, the Hyperspectral Digital Image Collection Experiment (HYDICE) carried out by the US Naval Research Lab used 206 channels, and the Airborne Visible and Infrared Imaging Spectrometer (AVIRIS) flown by JPL used 63 channels. These developments in scanner technology, and in the subsequent processing of gathered spectral information through data handling, have provided the GER 63 Channel Dias (Digital Airborne Imaging Spectrometer) used in this study. This instrument is an airborne unit designed for acquisition of spectral information (e.g., environmental studies, geological mapping).

The potential of multi- and hyperspectral scanner data for geological mapping and identification of mineralised zones on the Earth's surface has long been recognised and has been tested in many parts of the world (e.g., Chang & Collins 1983, Lyon 1996, Hilikka et al. 1998). In Norway, however, only a few such studies have been carried out. These have mostly dealt with mapping of lineaments (e.g., Rindstad & Follestad 1982, Wester et al. 1990, Roberts & Karpuz 1995), surficial deposits, and natural and anthropogenic pollution of soil and vegetation (e.g., Bølviken et al. 1977, Rød 1992). As a basis for evaluation of the remote sensing multispectral airborne scanner data, laboratory and field testing of the reflectivity of minerals in rock samples has been carried out.

Methodology and results

On 18 July 1996, a flight over a Norwegian test area in the Førdefjord district was carried out using the Geophysical & Environmental Research Corporation's 63-channel scanner in a 31-channel digital mode (GER 63). The site covers the Engebøfjell area (Fig. 1), including the elongate, eclogitised, gabbroic intrusions containing enrichments in Ti and Fe (Korneliusen & Foslie 1985, Lutro & Ragnhildstveit 1996). The tests consisted of three parts:

- (1) Laboratory measurement of the reflectivity curves using the spectrometer at the Defence Research Laboratory (Forsvarets forsknings institutt, FFI);
- (2) Field measurement using a portable spectral radiometer (GER 3700);
- (3) Spectral data analysis of data collected with the airborne multispectral scanner.

Laboratory measurement of reflectivity

Spectral measurement of rock samples (Table 1) was carried out at the FFI laboratory using a Perkin-Elmer UV scanner. Each sample was treated separately and scanned in the

Sample no	Rock type	TiO ₂ (%)	Fe ₂ O ₃ (%)	Description of the rock samples
R1	leuco-eclogite	0.5	10	light coloured rock, no moss on surface
R2	leuco-eclogite	0.5	10	light coloured rock, no moss on surface
R3	leuco-eclogite	0.6	11.8	light coloured rock, no moss on surface
R4	leuco-eclogite	0.6	11.8	light coloured rock, no moss on surface
5R	ferro-eclogite	3.2	16.9	dark coloured rock, no moss on surface
R6	ferro-eclogite	3.2	16.9	dark coloured rock, no moss on surface
R7	ferro-eclogite	3.4	18	dark coloured rock, no moss on surface
R8	ferro-eclogite	3.4	18	dark coloured rock, no moss on surface
R9	ferro-eclogite	3	17	dark coloured rock, no moss on surface
R10	ferro-eclogite	3	17	dark coloured rock, some moss on surface
R11	gneiss			light coloured rock, no moss on surface
R12	gneiss			light coloured rock, no moss on surface
R13	gneiss			light coloured rock, some moss on surface
R14	gneiss			light coloured rock, no moss on surface
R15	gneiss			
R16	gneiss			

Table 1. Rock samples collected from Engebø in 1996 and analysed for contents of TiO₂ and Fe₂O₃ (given as wt. %).

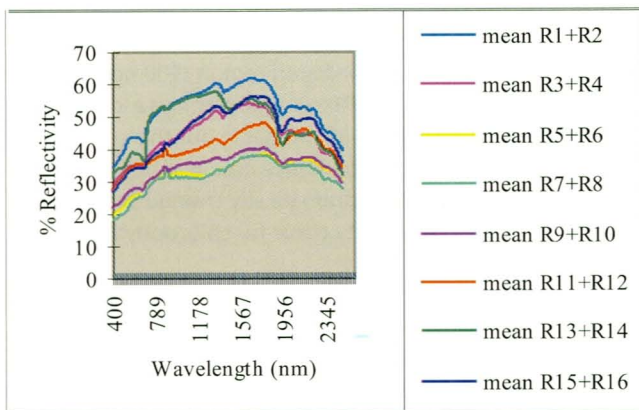


Fig. 2. Reflectivity (in %) of the main rock samples studied, compared to a standard of BaSO₄. R1 – R4: leuco-eclogite, R5 – R8: ferro-eclogite, R11-R16: gneiss.

waveband range of 480-3129 μm. Scanned data were standardised against Ba₂SO₄·2H₂O reference values and stored in ASCII format. Results are shown as a mean value of reflectivity (%) in the spectral band from 500 nm (= 0.5 μm) to 2400 nm. As seen in Fig. 2, % reflectivity values are up to 15 % higher for samples of leuco-eclogite (mean of R1+R2, mean of R3+R4) and gneiss (mean of R11+R12, mean of R13+R14, mean of R15+R16) compared with samples of ferro-eclogite (mean of R5+R6, mean of R7+R8, mean of R9+R10). Reflectivity data

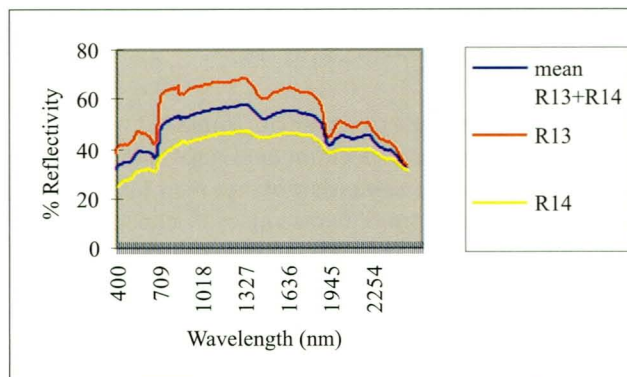
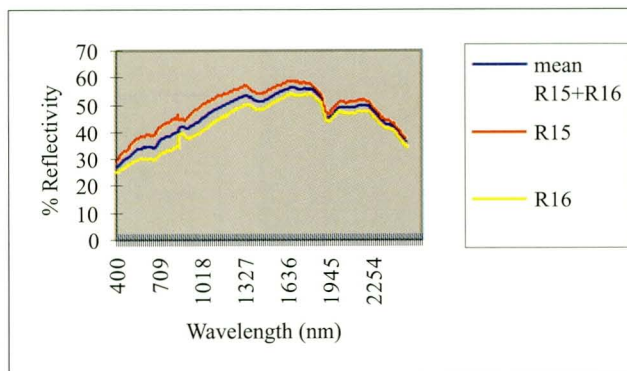
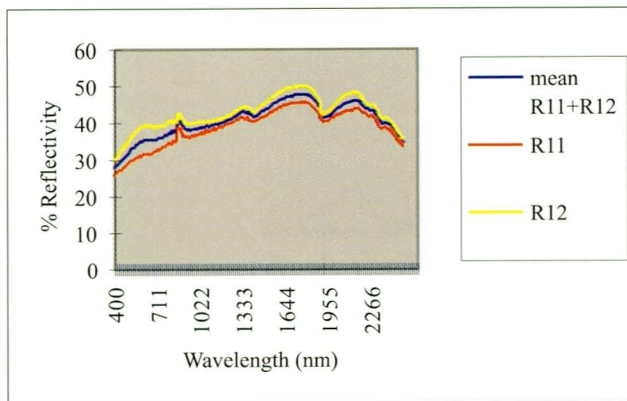


Fig. 4. Reflectivity (%) of sub-samples of a sample of gneiss, compared to the mean of each measurement. (top): Sub-samples R11, R12 and mean R11+R12, (middle): Sub-samples R15 and R16 and mean R15+R16, (bottom): Sub-samples R13 and R14 and mean R13+R14.

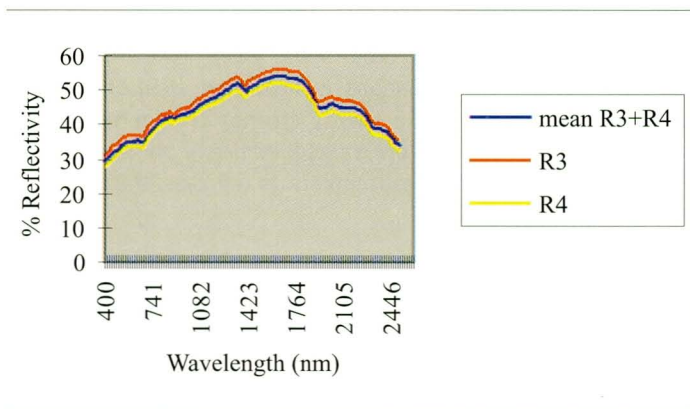
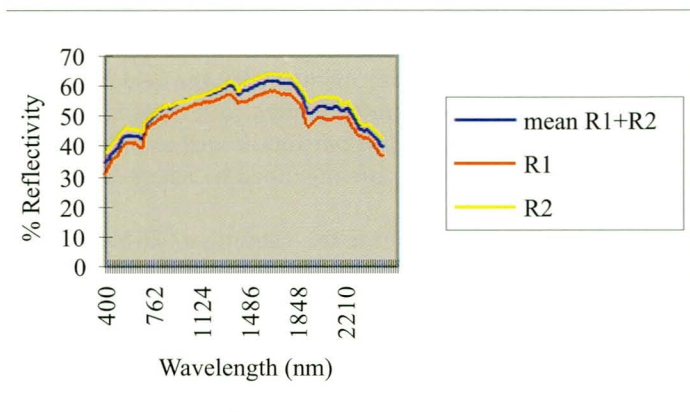


Fig. 3. (top): Reflectivity (%) of two sub-samples (R1, R2) of a sample of leuco-eclogite, compared to the mean of the measurement (R1+R2). (bottom): Reflectivity (%) of two further sub-samples of leuco-eclogite (R3, R4) compared to the measurement mean (R3+R4).

across the wavelength band are presented in a series of spectra allowing more detailed interpretation of the data (leuco-eclogite, Fig.3; gneiss, Fig. 4 and ferro-eclogite, Fig. 5). Sample numbers and contents of TiO₂ and Fe₂O₃ are given in Table 1. Spectral patterns are lithology-specific, and significant differences in TiO₂ and Fe₂O₃ contents, for example among leuco-eclogites (Fig. 3), give curves with similar patterns and peaks (the two samples of leuco-eclogite have TiO₂ and Fe₂O₃ values of 0.5, 10 and 0.6, 11.8 wt. %, respectively).

Reflectivity spectra for typical gneisses are shown in Fig. 4. Curves R11 and R12 are sub-samples from the same bulk sample and are nearly identical. However, the spectra apparently differ little from leuco-eclogites (compare with Fig. 3). Gneiss sample R15 and R16 show the same reflectivity values

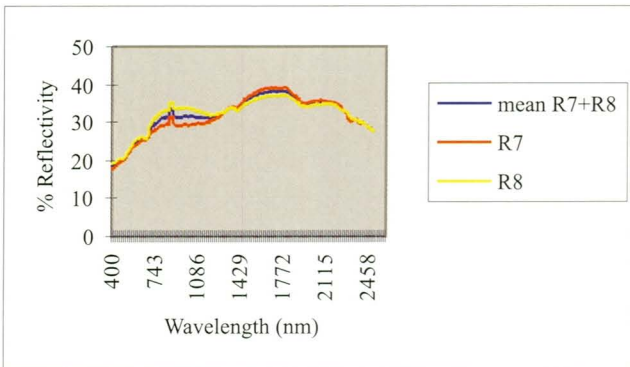
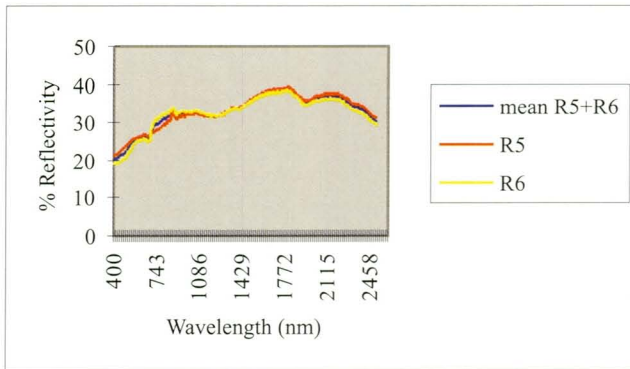


Fig. 5. (top): Reflectivity (%) of two sub-samples (R5, R6) of a sample of ferro-eclogite, compared to the mean of the measurement (R5+R6). (bottom): Reflectivity (%) of two further sub-samples of ferro-eclogite (R7, R8) compared to the measurement mean (R7+R8).

in the visible part of the spectrum as sample R11. In the central part of the infrared spectrum (900–1800 nm), however, reflectivity values are somewhat higher than for the other gneiss samples. Spectra of two samples of gneiss, R13 and R14, with and without a surface covering of moss, are shown in Fig. 4 (bottom). Comparison of these curves clearly demon-

strates that the reflectivity of sample R13 is affected by the presence of moss. A characteristic feature of the spectra is a sharp gradient in the near-infrared region (900 nm), characteristic for chlorophyll. The R14 sample displays a less marked reflectivity increase in the 900 nm band, but this sub-sample has less moss on the surface. These data indicate that moss on the sample surface will dramatically change the % reflectivity and give the reflectivity curve for chlorophyll (i.e. vegetation).

Four sub-samples of ferro-eclogite from two sites, R5/R6, with TiO₂ and Fe₂O₃ contents of 3.2; 16.9 % and 3.4; 18.9 %, and a second pair, R7/R8, were tested (Fig. 5). These samples show rather similar reflectivity spectra. Reflectivity curves for ferro-eclogite are characterised by rather low reflectivity values (ca. 20 %) in the visible part of the spectrum. Compared with the spectra for both leuco-eclogite and gneiss, this is a 10% reduction. The reduction of reflected energy is seen both in the visible and in the infrared parts of the spectrum.

Field measurement using a portable spectral radiometer (GER 3700)

The GER Mark V spectrometer is a portable instrument for measuring reflected electromagnetic energy. It operates in the visible and infrared parts of the spectrum, from 300 to 2500 nm (or 0.3 to 25 μm). The spectral resolution is 10 nm, with a sampling interval of 2 nm. A BaSO₄ plate is used as a standard for the instrument, and the BaSO₄ values are given together with the spectral readings at the measured site. This BaSO₄ standard allows for normalisation of site readings which, as will be explained later, is important. The field study was intended to demonstrate if different rock types in the area could be differentiated at outcrop as well as in hand specimen. Such applications are described by Kale & Rown (1980).

The working spectral range of the instrument GER Mark V covers the same wavelength region as the GER 63-channel imaging spectrometer, operating in 31-channel mode, which was flown over the area in July 1996. Due to logistical problems, fieldwork using the GER Mark V spectrometer was not carried out until 11 August 1996. At this time of the year, however, the variations in incoming electromagnetic energy are not considered to have any major influence on spectral measurements. In our case, the time

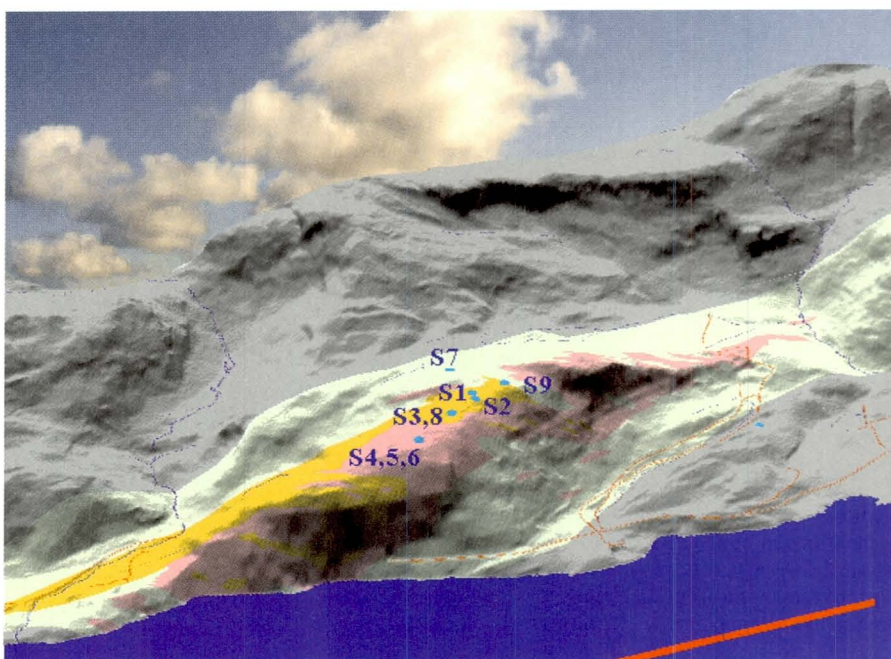


Fig. 6. 3-dimensional image of Engebøfjell showing the major rock units and locations of samples used for reflectivity data. The central part of the image shows ferro-eclogite (violet), leuco-eclogite (yellow), amphibolite (light green) and gneiss (grey). The red line indicates a distance of 1 km. The model was constructed using the Intergraph Voxel Analyst program, with grid resolution 5 x 5 m.

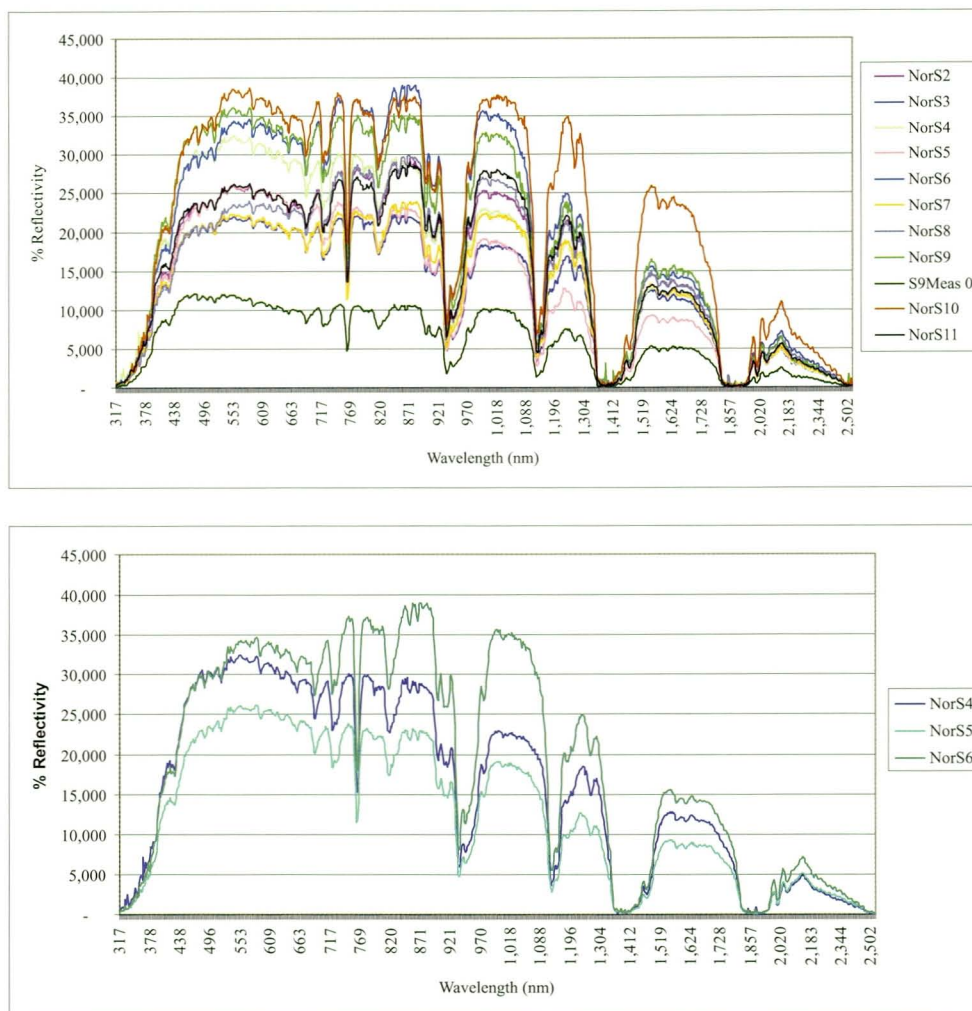


Fig. 7. (top): All readings illustrated by a single sample from each sample site S2 –S11, see Fig 6. The readings for the sample sites of the different rocks cannot be readily distinguished from one another. (bottom): Spectra from three samples sites, S4 to S6, of ferro-eclogite.

of the day when the measurements were taken (from 08.40 to 15.33), together with the air humidity, constitute greater sources for deviation. No corrections were made for potential changes in measurement due to day and month. Field sites are shown in Fig. 6 and tabulated in Table 2. Spectra for leuco-eclogite (S2, S3), ferro-eclogite (S4, S5, S6), amphibolite (S7, S8) and gneiss (S9) are shown in Fig. 7a. Minor differences between the different rock types are noted, yet variation between rock types of the same type is often greater, allowing little discrimination.

As an example, readings of massive ferro-eclogite were made at sample localities S4, S5 and S6 (Fig. 7). TiO_2 and Fe_2O_3 contents (in wt. %) of ferro-eclogite at the three sites were 4.27, 14.28; 4.03, 13.95; and 4.36, 12.93, respectively. All three localities had some surface moss. The three curves show some considerable variation, readings varying both with the extent of moss cover, but also significantly with the time of day when the measurements were taken. The information base available from the field measurements indicates that the moss cover constitutes the greatest influence on reflectivity and strongly impacts on differentiation of rock types. The rock surface of ferro-eclogite appears to have a somewhat higher reflectivity in the region 1180 - 1948 nm, whereas in the wavelength 2000 - 2497 nm, the reflectivity of this lithology is generally lower. The distinct and characteris-

tic features in the 1180 - 1948 nm band cannot, however, be used for differentiation of eclogite types using airborne measurements since the available channels for the GER 68 system do not cover the 1180 nm - 1948 nm region of the spectrum (see Table 3).

Airborne spectral scanning

The GER 63-channel imaging system is a multispectral airborne spectrometer. Measurements are carried out in the ultraviolet, visible, infrared and thermal parts of the spectra. The maximum number of channels for use in the scanner system is 63. In the tests reported here, 31 channels have been in operation mode and one channel (32) is used for gyro; the channels used are listed in Table 3. The thermal channels (channels 29, 30 and 31) might here be used for discrimination, as will be shown later.

The data have been subject to minimal preliminary processing. Basic data processing consists of gyro, baseline correction and panoramic corrections. Gyro correction is carried out to remove the effects of the aircraft motion by translating each scan line horizontally in space by an amount proportional to the number of gyro counts. The gyroscope encodes the amount of aircraft roll in the last channel. In the image, straight features within the image, such as roads, are straight, but the edges of the image may have irregular

Locality	Rock	% TiO ₂	% Fe ₂ O ₃	UTM-East	UTM-North	Spectral measurement , Engebøfjell, 11.aug. 1996				
						Measurement	Level [m]	40 dB Detector	Time	File name
S1	Leuco-eclogite	1.23	11.74	310589	6823337	0	0,6	OFF	09.33	S1M0.SIG
S1	Leuco-eclogite	1.23	11.74	310589	6823337	1	0,6	OFF	09.35	S1M1.SIG
S1	Leuco-eclogite	1.23	11.74	310589	6823337	2	0,6	ON	09.39	S1M2.SIG
S1	Leuco-eclogite	1.23	11.74	310589	6823337	4	0,6	OFF	09.49	S1M4.SIG
S1	Leuco-eclogite	1.23	11.74	310589	6823337	5	0,6	ON	09.56	S1M5.SIG
S2	Leuco-eclogite	1.17	12.14	310587	6823307	0	0,6	OFF	10.15	S2M0.SIG
S2	Leuco-eclogite	1.17	12.14	310587	6823307	1	0,6	OFF	10.20	S2M1.SIG
S3	Leuco-eclogite	1.16	10.66	310490	6823273	0	0,6	OFF	10.39	S3M0.SIG
S3	Leuco-eclogite	1.16	10.66	310490	6823273	1	0,6	OFF	10.44	S3M1.SIG
S4	Ferro-eclogite	4.27	14.28	310350	6823191	0	0,6	OFF	11.01	S4M0.SIG
S4	Ferro-eclogite	4.27	14.28	310350	6823191	1	0,8	OFF	11.05	S4M1.SIG
S5	Ferro-eclogite	4.03	13.95	310350	6823184	0	0,8	OFF	11.26	S5M0.SIG
S5	Ferro-eclogite	4.03	13.95	310350	6823184	1	0,8	OFF	11.31	S5M1.SIG
S6	Ferro-eclogite	4.36	12.93	310348	6823187	0	0,7	OFF	11.14	S6M0.SIG
S7	Amphibolite			310575	6823470	0	0,6	OFF	11.55	S7M0.SIG
S7	Amphibolite			310575	6823470	1	0,6	OFF	11.57	S7M1.SIG
S7	Amphibolite			310575	6823470	2	0,6	OFF	12.00	S7M2.SIG
S8	Amphibolite			310578	6823472	0	0,8	OFF	12.06	S8M0.SIG
S8	Amphibolite			310578	6823472	1	0,8	OFF	12.08	S8M1.SIG
S8	Amphibolite			310578	6823472	2	0,8	OFF	12.12	S8M2.SIG
S8	Amphibolite			310578	6823472	3	0,8	OFF	12.15	S8M3.SIG
S9	gneiss			310695	6823340	0	0,6	OFF	08.39	S9M0.SIG
S9	gneiss			310695	6823340	1	0,6	OFF	08.45	S9M1.SIG
S9	gneiss			310695	6823340	2	0,6	OFF	08.56	S9M2.SIG
S9	gneiss			310695	6823340	3	0,6	OFF	09.00	S9M3.SIG
S9	gneiss			310695	6823340	5	0,6	OFF	09.02	S9M5.SIG
S9	gneiss			310695	6823340	6	0,6	OFF	09.05	S9M6.SIG
S9	gneiss			310695	6823340	7	0,6	ON	09.08	S9M7.SIG
S9	gneiss			310695	6823340	8	0,6	ON	09.11	S9M8.SIG

Table 2. Sample localities for field investigations, 11th August 1996.

boundaries due to aircraft roll. Each scan line is translated by an integral number of pixels to the right or left; there is no re-sampling. The spectral content of the data is not affected by gyro correction. Baseline correction utilises on-board reference panels to normalise the effects of detector reference voltages. When targets with extreme radiance differences are imaged, the GER scanner utilises a time-varying reference voltage to increase the effective dynamic range. The image of the baseline strip records the digital counts of a constant-reflectance panel. In baseline correction, the reference panel images are used to normalise the data so that the constant-reflectance panels have a constant digital count in the image. Each line and each channel are normalised individually. The 32 baseline pixels are then removed from the data set.

Panoramic correction corrects the geometric distortions

caused by the different viewing geometry in different parts of each scan line. Pixels are re-mapped into their correct position using nearest-neighbour re-sampling where possible, and linear interpolation where new pixels must be created. The spectral content for the nearest-neighbour pixels is not affected by this correction. The data sets are received as 8 mm (Exabyte) tape. It should, however, be noted that the chosen channels (Table 3) do not favour detection and differentiation of ferro-eclogite in the 1000 nm - 1948 nm of the spectrum, as there is only one channel (14) within this range.

ENVI software (Environment for Visualizing Images version 2.7) is used for image processing and classification of multispectral analysis based on the aircraft remote sensing data. The image processing system (ENVI) uses a generalised raster data format stored as a binary stream of bytes in band-

Channel	Band (nm)
1	410.00
2	432.00
3	483.6
4	521.3
5	565.8
6	617.7
7	665.8
8	716.6
9	768.5
10	823.7
11	883.90
12	941.9
13	989.7
14	1048.3
15	2039.3
16	2084.00
17	2112.5
18	2145.2
19	2170.00
20	2208.00
21	2237.7
22	2270.7
23	2296.2
24	2333.3
25	2358.00
26	2388.6
27	2411.7
28	2446.9
29	9468.4
30	10206.5
31	10983.1
32	Gyro

Table 3. Wavelength calibration for GER 63-Channel Sensor in 31-Channel operation.

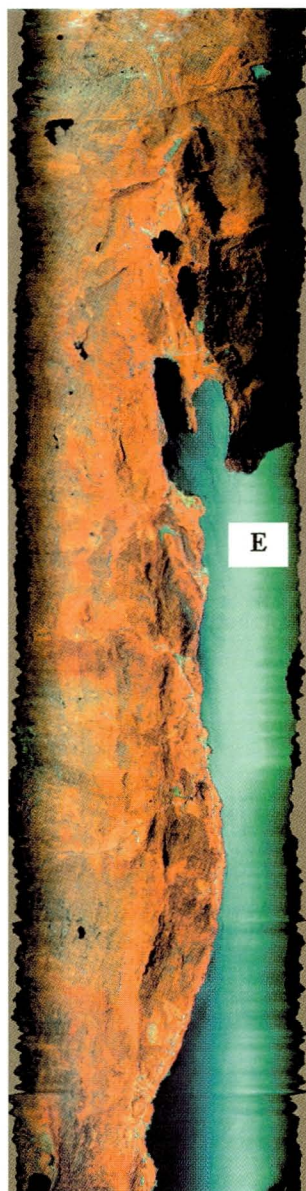


Fig. 8. Test flight line 1. The Engebø test area is shown as an RGB-colour image. Channel 13: red, Channel 6: green, Channel 4: blue. Engebøneset is marked with E.

sequential (BSQ) format. The basic function starts with an open image file where the different bands can be presented alone as a grey scale image, or combined, as an RGB-colour image (Fig. 8). This gives us the possibilities of combining channels 2 (blue), 5 (green) and 9 (red) and thus creating a false colour image for the areas cover by the flight line 1 (Fig. 1). This colour combination shows that the area is heavily vegetated as the reflected infrared from channel 9 dominates the image. Blue and green colours are chosen for channels 2 and 5 with low reflectivity due to absorption by chlorophyll. The blue/green colours thus show areas of bare rock; the fjord would have no chlorophyll in this context. From Fig. 8, it is only in the elevated parts of the area that a bare rock-surface, with little or no vegetation, is present.

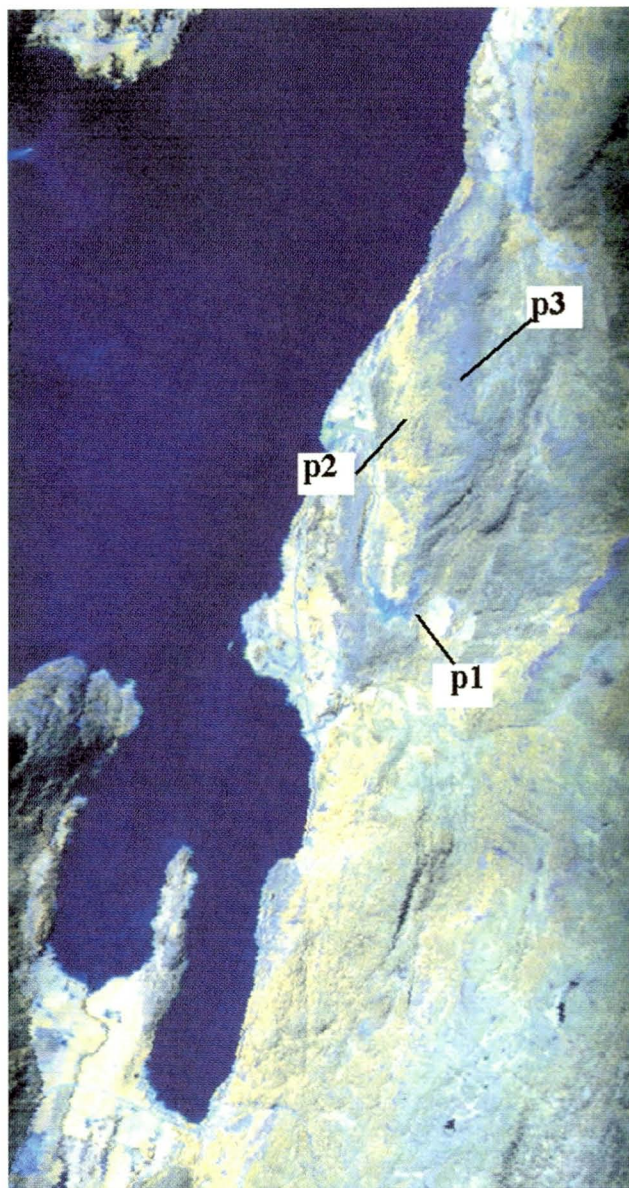


Fig. 9. Barren rock surface (p1), nearly barren surface (p3) and an area dominated by vegetation (p2) are shown in a spectral plot (see Fig. 12).

In the immediate vicinity of Engjebøfjell (Fig. 1), such areas only form a small proportion of the total area, based on a RGB-composite of channels 5, 8 and 13 constructed from data from flight line 4, shown in Fig. 9. The variance in the spectral reflectivity on all 31 channels from test sites visited in the field representative of nearly barren rock surface (p1), barren rock surface (p2) and an area dominated by vegetation (p3) are shown (Fig. 10). It is clearly shown that the heavily vegetated site (p2) has a maximum of reflection in channel 10, equal to 823 nm. The barren rock surfaces on the other hand (p1 and p2) show maximum values in channel 4, equal to 521 nm. In the areas from 1500 to 2400 nm, the curves of reflections are quite similar. In the thermal channels (channels 29, 30 and 31), however, there seems to be a higher value of thermal radiation for barren rock samples. This might be explained as a result of the trapping of radiant energy (green-

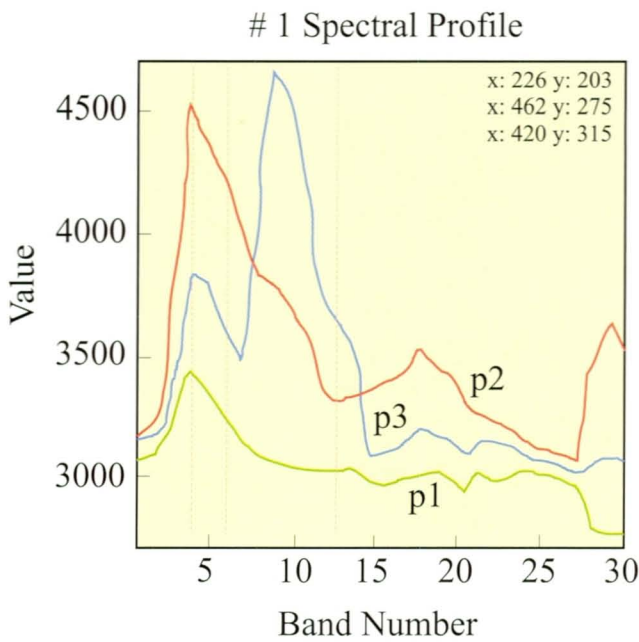


Fig. 10. RGB-composite of channels 5, 8 and 13, scanner flight 4 (Fig. 1), with location marks of spectral plots shown in Figs 7-9.

house effect) under a cover of leaves. Thermal radiation might, as will be discussed later, be one channel of information which permits a classification of surface type.

A classification of the region of interest (ROI) was made on the test flight 4 data. The classification menu in ENVI software gives access to supervised and unsupervised classification. Utilities are also provided for end-member collection, classifying previous rule images, calculating class statistics, etc. Supervised techniques use the end member collection utility to import training class spectra; ENVI's integrated region-of-interest (ROI) selection utilities are used to interactively define training classes. The selection routines allow extraction of training statistics from polygons, vectors, etc.

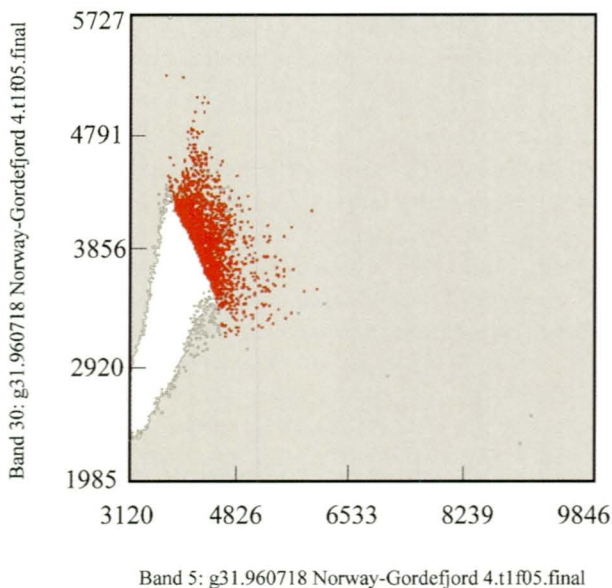


Fig 11. Scatter plot of the minimum noise fraction (MNF) transformation used to determine the inherent dimensionality of channels 5 and 30.

The minimum noise fraction (MNF) transformation can be used if a quick classification is required, as in our case. This transformation is used to determine the inherent spectral dimensionality of image data, to segregate noise in the data, and to reduce the computational requirements for subsequent processing (Boardman & Kruse 1994).

In our work, the channel information for barren rock or nearly barren rock surfaces (marked with p1, p3; Fig. 10) and vegetation (p2; Fig. 10) is used as separation criteria. Expression of these properties can be presented in terms of a two-dimensional diagram plotting data from channel 5 against the thermal channel 30 (Fig. 11).

In the algorithms on which this diagram is based, different transformations are carried out. The first transformation is based on an estimated noise covariance matrix, which decorrelates and re-scales the noise in the data. This results in transformed data in which the noise has unit variance and no band-to-band correlation. The second transformation is a standard principal components transformation of the noise-whitened data. Thus, the data space can be divided into one part assisted with large eigen-values and coherent eigen images, and a complementary part with near-unity eigen-values and noise-dominated images. Classifying the data set by marking the area of interest by a 'trial and error procedure' allows a best fit to be made. In Fig. 11, the selected data-points are shown (in red) and superimposed onto the colour image of the area in Fig. 12. It can be seen that this classification easily picks out the non-vegetated areas. These areas, which include roads as well as bare rock surfaces, are readily seen. A comparison of the areas with gneiss and leuco-eclog-

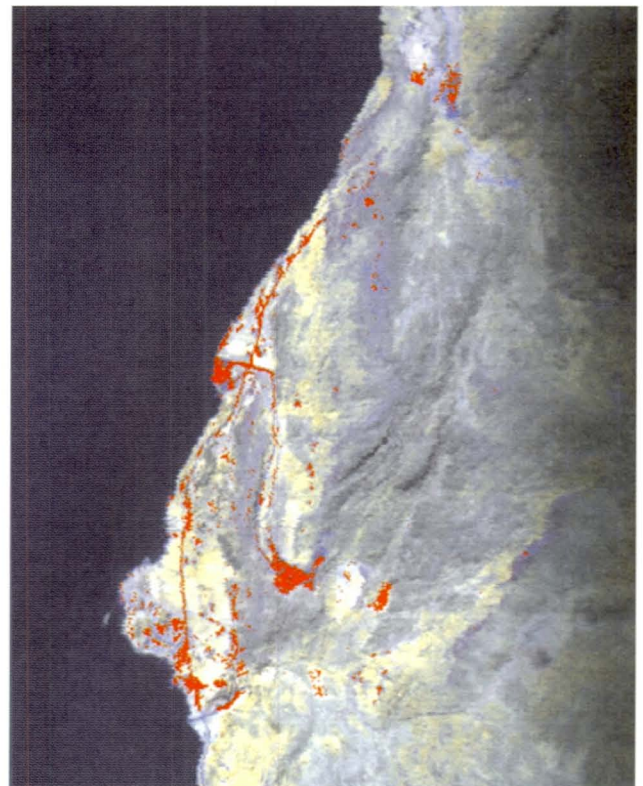


Fig. 12. The region of interest with the scatter plot from Fig. 11 superimposed onto it.

ite shows, however, that there is no significant separation of the different rock types.

Conclusions

The laboratory tests indicate that the rock surfaces of ferro-eclogite will generally have a lower reflectivity compared with the surface of both leuco-eclogite and gneiss. However, the presence of moss on the rock surface will change these characteristics significantly. The data collected in the field emphasise the fact that vegetation cover and measurement conditions impact heavily on the results. However, the findings do suggest that different % reflectivity values in distinct parts of the spectrum could possibly be used as a tool to discriminate between areas characterised by gneiss, leuco-eclogite and ferro-eclogite, if other factors influencing the data are carefully considered. However, the unavailability of the 1180-1948 nm band for airborne measurement makes application of a part of these differences of considerable interest, yet of little practical benefit, when applying the methods as a prospecting tool using GER 63 data. Other sensors such as HYMAP do cover these wavelengths and have great potential.

The airborne scanner data and interpretation thereof are useful in that they reveal a means to discriminate between areas of vegetation and bare rock surface. However, the area is too heavily vegetated for closer separation based on a scanner resolution of 10 m x 10 m. The airborne techniques are less successful in distinguishing different rock types, at least leuco- from ferro-eclogite. Adoption of more suitable channels, covering that part of the spectra in which differences between rock types have been identified in both laboratory and field studies, would give more useful information. Small-scale variations in vegetation cover and moss density are, however, a concern and may preclude more routine application of such techniques in prospecting.

Acknowledgements

We wish to thank Benny Moeller Soerensen (GER-INTRADAN A/S) and the late Prof. Brian Sturt for valuable co-operation; and Dr. Stuart Marsh for his critical reading of an earlier version of the manuscript.

References

- Boardman, J. & Kruse, F. 1993: Knowledge-based geologic mapping with imaging spectrometers: *Remote Sensing Reviews* (special issue on NASA Innovative Research Program (IRP) results), 8, 3-28.
- Bølviken, B., Honey, F., Levine, R., Lyon, R. & Prelat, A. 1977: Detection of natural heavy-metal-poisoned areas by Landsat-1 digital data. *Journal of Geochemical Exploration* 8, 457-471.
- Chang, S. & Collins, W. 1983: Confirmation of the Airborne Biogeophysical Mineral Exploration Technique Using Laboratory Methods. *Economic Geology* 78, 723-736.
- Hilkka, A., Ruohomaki, T., Raino, H. & Laitinen, J. 1998: Application of AISA airborne imaging spectrometer to the discrimination of Quaternary soil types in the Mantsala-Ohkola area in Finland. *Geological Survey of Finland Report RS/1998/4*.
- Kale, A. B. & Rown, L.C. 1980: Evaluation of multispectral middle infrared aircraft images for lithologic mapping in the east Tintic Mountains, Utah. *Geology* 8, 234-239.
- Korneliusson, A. & Foslie, G. 1985: Rutile-bearing eclogites in the Sunnfjord region of Western Norway. *Norges geologiske undersøkelse Bulletin* 402, 65-71.
- Lutro, O. & Ragnhildstveit, J. 1996: Geological map of the Førdefjord area, bedrock map, scale 1:50,000. (unpublished). *Norges geologiske undersøkelse*.
- Lyon, R. 1996: Spectral Properties of Minerals – Significant in Mineral Exploration and Environmental Studies. *Eleventh Thematic Conference Remote Sensing, Las Vegas, Nevada, USA*.
- Richards, J.A. & Jia, X. 1999: *Remote Sensing Digital Image Analysis, 3rd edition*. Springer-Verlag Berlin Heidelberg New York.
- Rindstad, R. & Follestad, B.A. 1982: Digital methods for lineament analysis. First Thematic Conference: Remote Sensing of Arid and Semi-Arid Lands, Cairo, Egypt. *Environmental Res. Ins. Mich. Ann Arbor, Michigan, United States*, 1982, 955-961.
- Roberts, D. & Karpulz, M.R. 1995: Structural features of the Rybachi and Sredni Peninsulas, Northwest Russia, as interpreted from Landsat-TM imagery. *Norges geologiske undersøkelse Special Publication* 7, 145-150.
- Rød, J.K. 1992: Perspektivisk visualisering av et SPOT-bilde samregistrert med geologisk tema. *Norges geologiske undersøkelse Report* 92.256.
- Wester, K., Lunden, B. & Bax, G. 1990: Analytically processed Landsat TM images for visual geological interpretation in northern Scandinavian Caledonides. *ISPRS Journal of Photogrammetry and Remote Sensing* 45, 443-459.